Materials Characterization 106 (2015) 11–19

Contents lists available at ScienceDirect

Materials Characterization

journal homepage: www.elsevier.com/locate/matchar

Characterization of carbon ion implantation induced graded microstructure and phase transformation in stainless steel

Kai Feng [a], Yibo Wang [a], Zhuguo Li [a,*], Paul K. Chu [b,*]

[a] Shanghai Key laboratory of Materials Laser Processing and Modification, School of Materials Science and Engineering, Shanghai Jiao Tong University, Shanghai 200240, China
[b] Department of Physics and Materials Science, City University of Hong Kong, Tat Chee Avenue, Kowloon, Hong Kong, China

ARTICLE INFO

Article history:
Received 4 February 2015
Received in revised form 21 April 2015
Accepted 28 April 2015
Available online 30 April 2015

Keywords:
Stainless steel
Ion implantation
Transmission electron microscopy
Grazing incidence X-ray diffraction
Corrosion

ABSTRACT

Austenitic stainless steel 316L is ion implanted by carbon with implantation fluences of 1.2×10^{17} ions-cm^{-2}, 2.4×10^{17} ions-cm^{-2}, and 4.8×10^{17} ions-cm^{-2}. The ion implantation induced graded microstructure and phase transformation in stainless steel is investigated by X-ray diffraction, X-ray photoelectron spectroscopy and high resolution transmission electron microscopy. The corrosion resistance is evaluated by potentiodynamic test. It is found that the initial phase is austenite with a small amount of ferrite. After low fluence carbon ion implantation, an amorphous layer and ferrite phase enriched region underneath are formed. Nanophase particles precipitate from the amorphous layer due to energy minimization and irradiation at larger ion implantation fluence. The morphology of the precipitated nanophase particles changes from circular to dumbbell-like with increasing implantation fluence. The corrosion resistance of stainless steel is enhanced by the formation of amorphous layer and graphitic solid state carbon after carbon ion implantation.

1. Introduction

Austenitic stainless steels are widely used in countless engineering applications due to their reasonable corrosion resistance and relatively low cost [1,2], but local corrosion, especially intergranular corrosion, in stainless steels can seriously degrade the mechanical performance such as strength and ductility [3,4]. Intergranular corrosion is caused by Cr depletion in the vicinity of Cr-rich M23C6-type precipitates at grain boundaries [5,6] and many strategies have been devised to improve the corrosion performance. It has been reported that interstitial alloying elements such as C and N can effectively stabilize the austenite phase and passive film in stainless steels consequently improving the strength, wear resistance, and corrosion resistance without significantly reducing the ductility [6–9].

Ion implantation is a versatile and powerful technique broadly applied to alter the surface properties of different types of materials [10–14]. Although metallic carbides, especially Cr carbides, are considered detrimental components in stainless steels inducing intergranular corrosion, carbon ion implantation has attracted considerable attention because no carbides are produced during the treatment [15]. Follstaedt et al. [16] found that carbon ion implantation could amorphize stainless steels containing 12%–18% Cr, because the Cr in stainless steels could interact with C to stabilize the amorphous phase. Hong et al. [17] pointed out that the amorphized carbon-implanted layers were composed of graphitic solid-state carbon. An amorphized and carbonaceous layer was formed on the surface after high fluence carbon ion implantation [18]. XPS showed the presence of C—C bonds in the ion-implanted samples, suggesting the formation of a graphitic layer on the surface [19]. Murphy et al. [20] reported the presence of two amorphous layers separated by a layer of expanded austenite after 5×10^{17} C ions-cm^{-2} ion implantation. The selective amorphization in the near-surface is supposed to be directly related to the energy released by the implanted carbon ions, while the expanded austenite is a result of the carbon ions coming to rest in an interstitial position in the austenitic cell. Although the surface structure of carbon ion-implanted stainless steel has been investigated peripherally, the structural evolution in stainless steels during carbon ion implantation has been scarcely conducted systematically. Additionally, the corrosion behavior of C ion-implanted stainless steels has been rarely investigated so far. In the work described here, the evolution of the surface structure as a result of carbon ion implantation is studied systematically by X-ray diffraction (XRD), X-ray photoelectron spectroscopy (XPS), and high-resolution TEM and the corresponding corrosion behavior in 3.5 wt.% NaCl is also investigated.

2. Material and methods

2.1. Substrate materials

Commercial stainless steel 316L (SS316L) plates supplied by Trinity Brand Industries, Inc. were used in the experiments. The main initial phase was austenite with grain sizes between 5 and 20 μm. The stainless steel plates were mechanically polished by SiC 1200 grade sandpaper,

* Corresponding authors.
E-mail address: lizg@sjtu.edu.cn (Z. Li).

http://dx.doi.org/10.1016/j.matchar.2015.04.019
1044-5803/

cleaned with acetone and distilled water in an ultrasonic cleaner, and dried.

2.2. Ion implantation

Carbon ion implantation was carried out in the HEMII-80 High Energy Metal Ion Implanter with a MEVVA ion source in the Plasma Laboratory of City University of Hong Kong. The base vacuum in the implantation chamber was below 5.0×10^{-5} Pa. A 99.9% pure carbon source produced the plasma which was extracted and accelerated to 40 keV. The implantation fluences were 1.2×10^{17} ions-cm^{-2}, 2.4×10^{17} ions-cm^{-2}, and 4.8×10^{17} ions-cm^{-2}.

2.3. Characterization

After ion implantation, the surface crystallographic structure was characterized by grazing incidence X-ray diffraction (GIXRD) on a RIGAKU D/MAX 2550 diffractometer with Cu Kα radiation ($\lambda = 0.15406$) at room temperature. The incident angles were 0.5°, 1° and 1.5° and the step size was 0.02°.

The chemical states of C, Fe, Cr and Ni were determined by X-ray photoelectron spectroscopy (XPS) using a Kratos AXIS Ultra equipped with a monochromatic Al Kα radiation source operated at a constant pass energy of 11.75 eV, take-off angle of 45°, and a step size of 0.25 eV. The chemical states of C, Fe, Cr and Ni with different depths were obtained by 3 kV Ar sputtering of a 3×3 mm^2 area to ensure that artifacts from the crater walls and induced roughness were minimized. The binding energy of the elements was normalized by that of carbon, 284.8 eV.

The cross-sectional microstructures were examined by high-resolution transmission electron microscopy (HR-TEM) performed on the FEI TECHAI G^2 F20 and JEOL 2100F operated at 200 kV. The samples for cross-sectional observation were prepared by the following procedures. The thinned sample (ion implanted side facing inward) was bonded to a silicon wafer using epoxy resin glue. The sample was sliced perpendicularly along the plane of the implanted surface and mechanically ground down to a thickness of about 10 μm. Finally, the sample was ion milled near the bonding line using a Gatan 691 at small incident angles between 8° and 3°.

2.4. Electrochemical test

The potentiodynamic test was conducted on a Zahner Zennium electrochemical workstation to evaluate the effect of carbon ion implantation on the corrosion resistance of SS316L. The test solution is 3.5 wt.% NaCl at room temperature. A three-electrode system, in which the counter electrode was a platinum sheet, the reference electrode was saturated calomel electrode (SCE), the working electrode was sample, was employed in this study. The reference electrode was separated from the solution by a Luggin capillary to avoid anion contamination. Before the electrochemical test, the open circuit potential (OCP) versus time was recorded for 1 h to ensure electrochemical stability. Potentiodynamic polarization was performed at a potential scanning rate of 1 mV s^{-1}.

3. Results and discussion

3.1. XRD characterization

Fig. 1 presents the diffractograms of the SS316L sample implanted with 1.2×10^{17} and 4.8×10^{17} ions-cm^{-2} carbon measured at 0.5°, 1°, and 1.5° incident angles together with the XRD pattern acquired from the unimplanted SS316L for comparison. At incident angles of 0.5°, 1°, and 1.5°, the penetration depths of X-ray is estimated to be 26 nm, 81 nm, and 127 nm [21], respectively. The peak at 43.64° corresponding to austenite γ(111) is quite intense whereas the peak intensity at 44.5°

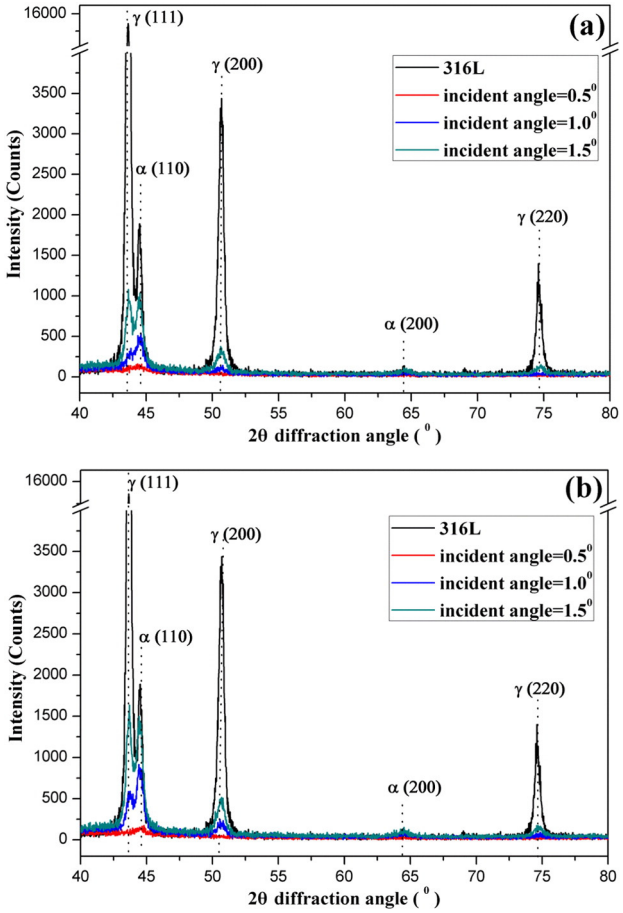

Fig. 1. GIXRD diffractograms in the 40–80° diffraction angles region acquired at incident angles of 0.5°, 1.0° and 1.5° from the unimplanted SS316L and carbon ion-implanted samples at 40 kV SS316L at fluences of (a) 1.2×10^{17} ions-cm^{-2} and (b) 4.8×10^{17} ions-cm^{-2}.

corresponding to ferrite α(110) is much less intense. The peaks at 50.7° and 74.6° correspond to austenite γ(200) and γ(220), respectively. Hence, the initial crystallographic structure of SS316L is composed of austenite and a small amount of ferrite. After carbon ion implantation, in the $2\theta = 42°$–45° region where the most intense diffraction peaks of austenite γ(111) and ferrite α(110) are located, the peaks at 0.5° disappear. Instead, a broad halo peak and background noise can be observed indicating that the implanted layer with a thickness of about 26 nm has been amorphized. At 1.0° incident angle, the austenite γ(111) peak shows reduced intensity and appears on the left side as a shoulder of the α(110) peak. This reflects an increase in the ferrite amount after carbon ion implantation. At an incident angle of 1.5°, the austenite γ(111) peak intensity increases and an additional peak at 64.5° is associated with α(200) stemming from ferrite formation. The evolution of the GIXRD patterns is almost the same as that implanted with 4.8×10^{17} ions-cm^{-2} of C. The thickness of the carbon ion implantation layer is about 240 nm as measured by XPS [22] and the crystallographic structure determined by GIXRD is thus within the implanted layer. Therefore, it is inferred that carbon ion implantation promotes the phase transformation from austenite to ferrite.

3.2. XPS analysis

The depth profiles acquired by XPS technique from carbon ion implanted SS316L with fluences of 1.2×10^{17} ions-cm^{-2}, 2.4×10^{17} ions-cm^{-2} and 4.8×10^{17} ions-cm^{-2} are shown in Fig. 2(a), (b) and (c), respectively. It can be seen that the carbon depth profile in these samples exhibits a Gaussian like distribution with a peak